Single photoelectron trapping, storage, and detection in a field effect transistor

doi: 10.1103/PhysRevB.67.045104

Single photoelectron trapping, storage, and detection in a field effect transistor

Hideo Kosaka,[1,*] Deepak S. Rao,[1] Hans D. Robinson,[1] Prabhakar Bandaru,[1] Kikuo Makita,[2] and Eli Yablonovitch[1]
[1]*Electrical Engineering Department, University of California at Los Angeles, Los Angeles, California 90095-1594*
[2]*Photonics and Wireless Device Research Laboratories, NEC Corporation, 34 Miyukigaoka, Tsukuba, Ibaraki 305-8501, Japan*
(Received 29 August 2002; published 17 January 2003)

We have demonstrated that a single photoelectron can be trapped, stored, and its photoelectric charge detected by a source/drain channel in a transistor. The electron trap can be photoionized and repeatedly reset for the arrival of successive individual photons. This single-photoelectron transistor, operating in the $\lambda = 1.3\ \mu$m telecommunication band, was demonstrated by using a window-gate double-quantum-well InGaAs/InAlAs/InP heterostructure that was designed to provide near-zero electron g factor. In general, g-factor engineering allows selection rules that would convert a photon polarization to an electron-spin polarization. Such a transistor photodetector could be useful for flagging the safe arrival of a photon in a quantum repeater. In the future, the safe arrival of a photoelectric charge would trigger the commencement of the teleportation algorithm in a quantum repeater to be used for quantum telecommunications.

DOI: 10.1103/PhysRevB.67.045104 PACS number(s): 85.35.Gv, 73.50.Pz, 85.35.Be, 78.67.De

Quantum information can take several different forms and it is beneficial as it is be able to convert among different forms. One form is photon polarization, and another is electron-spin polarization.

Photons are the most convenient medium for sharing quantum information between distant locations. Quantum key distribution[1] has been demonstrated by sending photons through a conventional optical fiber up to distances over 80 km.[2] As the distance increases, the secure data rate decreases, owing to photon loss. To expand the distance dramatically, it is necessary to realize a quantum repeater, which is based on quantum teleportation.[3] A quantum repeater requires quantum information storage,[4] and electron spin is a good candidate for such a quantum memory. We need to have a photodetector that converts from photon to electron, while transferring the quantum information from photon polarization to electron spin. This is sometimes called an entanglement preserving photodetector.[5] In addition, the photodetector must provide a trigger signal to flag the arrival of a photoelectric charge, and to commence the teleportation algorithm.

A field effect transistor (FET), and a single-electron transistor (SET) based on quantum dots, can both function as sensitive electrometers that can detect a single trapped electric charge. Our goal is to safely trap a photoelectron, so that its spin state can then be monitored. In this paper, we demonstrate the trapping and manipulation of individual photoelectrons, but we have not yet measured the trapped electron's spin properties. Previous experiments have demonstrated interband photon absorption resulting in the trapping of photo*holes*; on self-assembled InAs quantum dots,[6] or on DX centers,[7] near an FET source/drain channel. These produce positive photoconductivity, which is fairly common. The trapping of photo*electrons* is much more rarely observed, since it is accompanied by negative photoconductivity.[8]

Several kinds of photon effects on SET's made on modulation-doped semiconductors have been reported. Photon assisted tunneling is the most common effect. The tunneling takes place between an island and a source-drain reservoir,[9,10] between two adjacent islands,[11] or between an inner island and an outer ring split into Landau levels by a magnetic field.[12] In all these cases, the rather long photon wavelengths are controlled by the electron subband energy difference, rather than by the fundamental band gap as in our experiments.

These types of single-photon detectors should be distinguished from avalanche photodiodes, where the single-photon sensitivity arises from avalanche gain. In the FET and SET photodetectors, a single trapped electric charge can influence the current of millions of electrons in the source/drain channel. This is indeed the mechanism of ''photoconductive gain''[8] that is also sometimes called ''secondary photoconductivity.''[8] But this form of gain can also be considered as arising from transistor action. Thus the name ''single-photoelectron transistor'' (SPT) might be appropriate. Since the photoelectron is safely trapped, and is known to have a long spin lifetime in many semiconductors,[13] it can then be interrogated to determine its spin state. The initial goal is to monitor the photoelectric charge in such a way as to not disturb its spin state. Ultimately the goal is to measure its spin state as well.

At least three requirements should be satisfied to make a photodetector for quantum repeaters: (1) The wavelength that should be in the 1.3 μm or 1.55 μm, the low-loss window of optical fibers. (2) The sign of the photoconductivity that should be negative, which means the trapped information carrier should be an electron instead of a hole. (3) The electron g_e factor, which should be small, to make the up-and-down electron-spin states as indistinguishable as possible.[5] The first requirement suggests interband transition rather than intraband transition. The second requirement suggests creation of a positively charged trap for an electron. The third requirement is satisfied through g_e-factor engineering.[14,15]

The SPT that we present in this paper satisfies all of the above requirements. An InGaAs, quantum well is used with a band gap corresponding to $\lambda = 1.3\ \mu$m, as shown in Fig. 1. In Fig. 2 are shown the window-shaped circular gates that are negatively biased above the two-dimensional electron gas

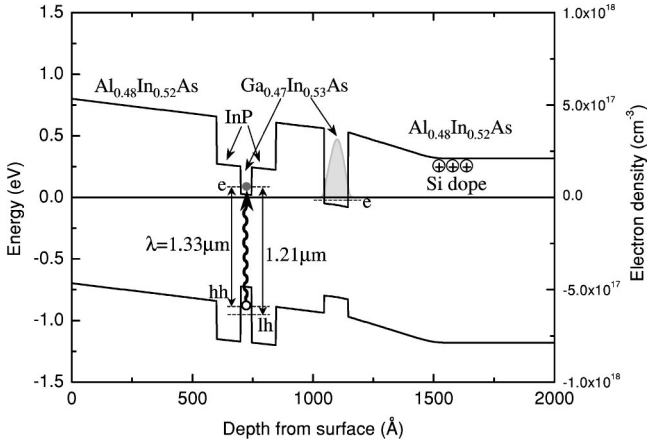

FIG. 1. The energy-band diagram of the single-photoelectron transistor (SPT) at zero bias simulated by using one-dimensional Poisson/Schrödinger equation. Photoinduced transitions between the heavy hole band and the conduction band are shown with an arrow. Photoionization of donors by $\lambda = 1.77$ μm light modulation dopes the channel. The tunneling time of trapped electrons in the top quantum well leaking to the bottom quantum well is estimated to be over 1 h by WKB simulation.

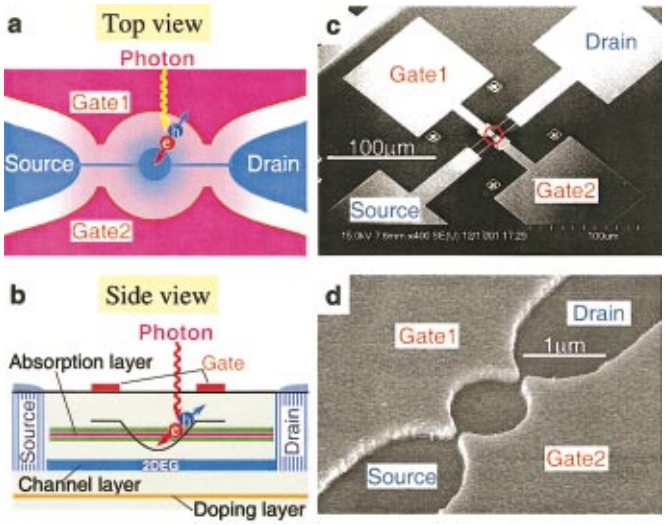

FIG. 2. (Color) A single-photoelectron transistor (SPT) with window-gate double-quantum-well modulation-doped heterostructure. (a) Top view of the window-gate part of the SPT. The center of the window gates is relatively positive to the surroundings when negative voltage is applied to the gates because of Fermi-level pinning. The blue regions indicate the two-dimensional electron gas (2DEG) in the channel layer. (b) Cross-section view of the layers in the SPT. The upper quantum well (QW) functions as an absorption layer and lower QW serves as a 2DEG channel layer, which is connected to source and drain. The curve on the absorption layer illustrates the electron potential when negative voltage is applied to the gates. (c) Scanning electron micrograph (SEM) picture of the SPT. (d) Close-up SEM picture of the window-gate part [circled part in (c)]. The window diameter is 1 μm.

(2DEG), leaving behind a relatively positive central island. The InGaAs absorption layer, which has a g_e factor $=-4.5$ in the bulk, is sandwiched between InP cladding layers of g_e factor $=+1.2$, to make the effective g_e factor in the absorption layer nearly zero. The measurements showed clear evidence for negative persistent photoconductivity steps. The abrupt drops in photoconductivity are strongly correlated with photon injection at the $\lambda = 1.3$ μm wavelength, leading to the conclusion that the SPT detects a single photon by sensing the charge of a safely trapped photoelectron in the absorption quantum well.

The photoabsorption layer is located above the source/drain channel layer, and both are made of $In_{0.53}Ga_{0.47}As$, separated by a high electron barrier layer made of $In_{0.52}Al_{0.48}As$ to prevent leakage. The source/drain channel layer is modulation doped and formed into a one-dimensional electron gas (1DEG) channel whose conductance is sensitive to the charge state of the island in the absorption layer above it. All layers were grown by gas-source molecular-beam epitaxy on semi-insulating InP, and consisted of a nominally undoped InP buffer layer 100-nm thick; an i-$In_{0.52}Al_{0.48}As$ buffer 1000-nm thick; a Si-doped ($5\times10^{17}/cm^3$) n-$In_{0.52}Al_{0.48}As$ doping layer 10-nm thick; an i-$In_{0.52}Al_{0.48}As$ lower spacer layer 30-nm thick; an i-$In_{0.53}Ga_{0.47}As$ channel layer 10-nm thick; an i-$In_{0.52}Al_{0.48}As$ barrier layer 20-nm thick; an i-InP cladding layer 10-nm thick; an i-$In_{0.53}Ga_{0.47}As$ absorption layer 4.5-nm thick; an i-InP cladding layer 10-nm thick; and an i-$In_{0.52}Al_{0.48}As$ capping layer 60-nm thick. The modulation-doped double-quantum-well structure creates a 2DEG in the lower-quantum well that is shaped into a 1DEG channel by the two split gates. The gates surround a circular window, 1 μm in diameter, that masks out unnecessary light exposure and fixes the potential at the edges surrounding the window. The Schottky gates, Al/Pt/Au, are fabricated using electron-beam lithography and electron-gun evaporation. The source/drain Ohmic contacts are made of AuGe/Ni/Au. Scanning electron microscope pictures of the whole device and the window gates are shown in Figs. 2(c) and 2(d), respectively. The energy-band diagram at zero bias, simulated by one-dimensional Poisson/Schrödinger equation, is shown in Fig. 1.

The sample is illuminated by monochromatic light through a large-core glass fiber that is carefully shielded to block any photons from the outer jacket. The light is created by a tungsten lamp and then filtered by a monochromator, a long-pass filter passing wavelength $\lambda > 1000$ nm, and a 30-dB neutral density filter. The optical power at the end of the fiber is measured by an InGaAs detector. The illumination area in the plane of the device is about 5 mm in diameter owing to light diffraction from the end of the fiber. Given the small device active area of 7.9×10^{-9} cm^2, defined by the 1-μm-diameter gate window, we estimate the actual light power in the active area to be 2.8×10^{-8} times smaller than the total power (assuming a Gaussian profile). The incident photon number is estimated by multiplying this scaling factor by the measured power divided by the photon energy.

By applying a negative voltage to the split window gates, the source/drain current through the channel layer is pinched off. Simultaneously, the applied negative voltage creates a two-dimensional potential minimum in the window at the absorption layer. This is because the surface Fermi level in

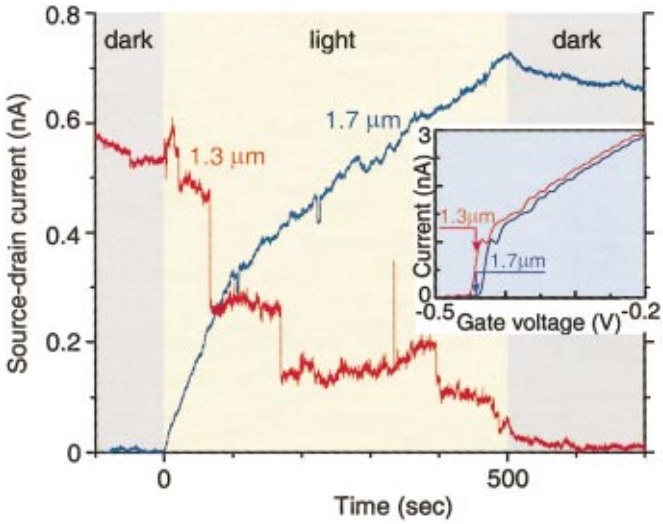

FIG. 3. (Color) Negative persistent photoconductivity of the SPT to $\lambda = 1.3\ \mu$m light starting with finite conductance, and positive photoconductivity at $\lambda = 1.7\ \mu$m light starting with zero conductance. The source-drain current drops in discrete steps when the SPT is exposed to $\lambda = 1.3\ \mu$m. The inset shows the initial current-gate voltage characteristics (I_{sd}-V_g curves) and bias points for the $\lambda = 1.3\ \mu$m exposure and the $\lambda = 1.7\ \mu$m exposure. The $\lambda = 1.3\ \mu$m photons create photoelectrons in the quantum well, which are trapped and pinch off the 2DEG, step by step. In contrast, $\lambda = 1.7\ \mu$m photoionizes the electrons and increases the 2DEG density. Photon number absorbed in the window area is 1 per second, on average.

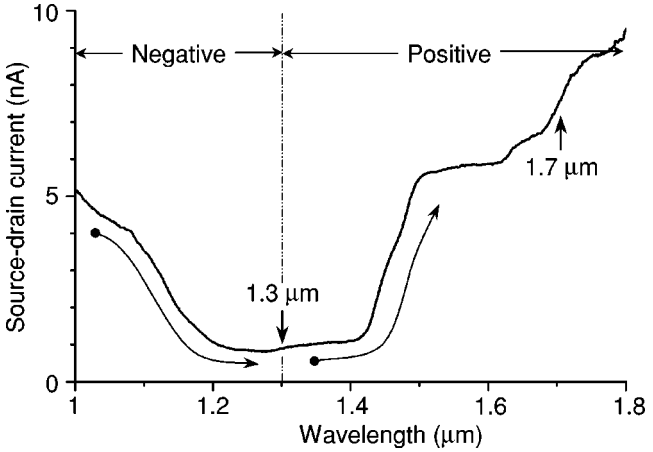

FIG. 4. Spectral dependence of the photoconductivity. The wavelength was swept from $\lambda = 1.0\ \mu$m to $\lambda = 1.8\ \mu$m while monitoring the source-drain current. From $\lambda = 1.0\ \mu$m to $\lambda = 1.3\ \mu$m, the current monotonically decreases, which is the range of negative photoconductivity. On the contrary, from $\lambda = 1.3\ \mu$m to $\lambda = 1.8\ \mu$m, the current monotonically increases with increasing wavelength, which is the range of positive photoconductivity. The crossover point, $\lambda = 1.3\ \mu$m, corresponds to the band gap in InGaAs quantum wells.

the circular area is pinned by the extrinsic surface states.[16] The electric field in the electrostatic potential well can separate an electron-hole pair created by a photon. The electron is attracted to the potential minimum at the center, and the hole is attracted to the negative gates as schematically shown in Fig. 2(b).

The source/drain current is measured at a constant voltage drop (V_{sd}) of 0.5 mV, at a temperature of 4.2 K. The interesting property of these photodetectors is that $\lambda = 1.77\ \mu$m light produces positive photoconductivity effectively doping the channel, and $\lambda = 1.3\ \mu$m light produces negative photoconductivity. We attribute the channel doping by $\lambda = 1.77\ \mu$m light to be due to photoionization of donors in the *n*-InAlAs doping layer. As a normal practice, we initially prepare the photodetectors for use by means of a deep soak in $\lambda = 1.77\ \mu$m light, to fully ionize the donors and to populate the source/drain channel. The pinch-off behavior in the source-drain conductance (I_{sd}-V_g curve) is shown in the inset of Fig. 3. The left-most I-V curve in that inset corresponds to full modulation doping after a deep soak in $\lambda = 1.77\ \mu$m light.

After the deep soak in $\lambda = 1.77\ \mu$m light to produce full channel doping, the gate voltage is adjusted for a current around 0.6 nA. The device is then exposed to a photon flux at a wavelength of $\lambda = 1.3\ \mu$m (red curve labeled 1.3 μm in Fig. 3). The photon exposure at $\lambda = 1.3\ \mu$m causes current to drop inexorably, step by step, except for occasional upward spikes. Thus as a result of trapped photoelectrons, the current is again pinched off, and the I_{sd}-V_g curve was shifted toward positive gate voltages as shown in the right-most curve of the inset in Fig. 3. At this pinch-off condition, if the device was again exposed to $\lambda = 1.77\ \mu$m, the channel current would be restored (blue curve labeled 1.7 μm in Fig. 3). The incident photon rate in the active window area for both wavelengths is about 100 photons/s. Since the absorptivity in the absorption layer is about 1%, on average 1 photon/s is absorbed in the window area. Thus the quantum efficiency for producing negative steps is estimated to be 1%.

The current drop for $\lambda = 1.3\ \mu$m means that the net negative charge is trapped near the source/drain channel. The occasional spikes we associate possibly with detrapping and retrapping of photoelectron, an effect that is seen also in Fig. 5. The difference in the magnitude of jumps in the current can be ascribed to the different positions where photoelectrons are trapped. Similar effects are seen for photohole[6,7] trapping. The exposure to $\lambda = 1.77\ \mu$m photons can energetically cause only photoionization, because the photon energy is smaller than any of the band gaps.

Detailed examination of the spectral dependence is not straightforward, since the channel conductance depends on the starting bias and the full prior history of spectral exposure. In Fig. 4, we start with an unpinched channel, and sweep wavelength starting from $\lambda = 1\ \mu$m up to $\lambda = 1.8\ \mu$m over an 80 s time period. First, the current monotonically decreases with increasing wavelength, corresponding to trapped electrons, with no further decrease at around $\lambda = 1.3\ \mu$m, the band gap of the InGaAs quantum wells. Negative trapped charge at wavelengths shorter than $\lambda = 1.3\ \mu$m is caused by photon absorption in the absorption layer or the channel layer. The photoelectrons in the conducting channel are mobile, and thus cannot contribute to trapped charge. Thus the negative steps must originate from photoelectrons produced in the absorption layer.

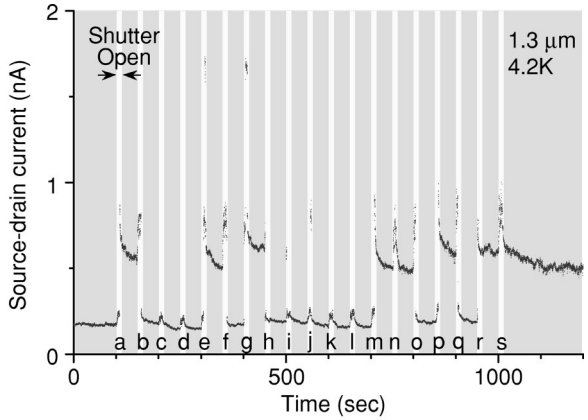

FIG. 5. Bitwise current state switching near the crossover from positive to negative photoconductivity. The photon source is gated to synchronize the current steps with the photons. The shutter was repeatedly opened for ~10 s every 50 s. The negative and positive photoconductivity events (electron trapping and photoneutralization) were balanced by incomplete soaking at $\lambda = 1.77\ \mu$m. The current alternates between a higher state and a lower state, the switching induced by optical pulses. In the dark, the state was stable for more than 1 h. The photon number absorbed within the window area is 30 photons in 10 s, on average.

By having an incomplete initial soak in $\lambda = 1.77\ \mu$m radiation, we can control the pinch-off voltage in between -0.5 V and $+0.1$ V. Now, when the pinch-off voltage is set nearly to zero, the $\lambda = 1.3\ \mu$m photocurrent still shows steps, but they are equally likely to be either positive or negative. The incomplete photoionization of donors in the initial state allows a balance between electron trapping and photoionization. To make this phenomenon clear, we periodically opened the optical shutter for 10 s in every 50 s, maintaining the SPT in a balanced condition biased at ~0 V. The resulting current pulses are shown in Fig. 5. The optical shutter is open during the time slots labeled a, b, c, etc., and closed during the intervening periods. Successive optical pulses usually produced either electron trapping or photoionization, alternating, depending on the previous state. Sometimes multiple optical pulses were required before the state would alternate. Within the 10-s optical pulse, there might be a transient thermal response, especially in time slot *g*; but that returned to either of the two alternating states after the optical pulse. The photon number absorbed in the window area is ~30 on average within the 10-s pulse. The estimated quantum efficiency is consistent with that in Fig. 3.

The switching behavior in Fig. 5 is due to photoelectron trapping/detrapping located either in (a) the shallow circular potential well between the window gates in the absorption layer, or (b) at donor sites. In case (b), the donors that could contribute to trapping/detrapping are the residual donors in the absorption layer rather than those in the modulation-doped layer. The modulation-doped donors, which are located far below the channel, would only produce a smooth increase in conductivity by photoionization as was seen in Fig. 3 for $\lambda = 1.77\ \mu$m light. In either case (a) or (b), there are two possible mechanisms for the positive steps in Fig. 5; photoionization of the trapped electron, or annihilation of the trapped electron by injected holes. The photoionization mechanism would require a specific photoionization cross section to be consistent with the rough equality between trapping and detrapping rates. On the other hand, annihilation by photoholes would require a hole trapping rate that is roughly coincident with the electron trapping rate. Such an adjustment may have been made by the adjustment of potential wells through the pinch-off voltage requirement of Fig. 5.

In conclusion, we have trapped, safely stored, and detected single photoelectrons in a window-gate double-quantum-well transistor structure. This single-photoelectron transistor detector satisfies three key requirements for a quantum repeater photodetector. It has an optical wavelength suitable for optical fibers, it safely traps and detects a single photoelectron, and the g_e factors can be designed to satisfy the requirements for an entanglement preserving photodetector. The wavelength could be shifted to $\lambda = 1.55\ \mu$m, which is more preferable, by using strain engineered substrates.[15] We believe that the quantum efficiency can be brought close to unity by optical cavity enhancement. We have yet to prove the entanglement transfer from photons to electrons, but we believe such a demonstration will be a breakthrough for realizing long-distance quantum key distribution or long-distance teleportation.

The project was sponsored by the Defense Advanced Research Projects Agency & Army Research Grants Nos. MDA972-99-1-0017 and DAAD19-00-1-0172. The content of the information does not necessarily reflect the position or the policy of the government, and no official endorsement should be inferred.

*On leave from Fundamental Research Laboratories, NEC Corporation.

[1] C.H. Bennett, F. Bessette, G. Brassard, L. Salvail, and J. Smolin, J. Cryptology **5**, 3 (1992).
[2] P.A. Hiskett, G. Bonfrate, G.S. Buller, and P.D. Townsend, J. Mod. Opt. **48**, 1957 (2001).
[3] C.H. Bennett, G. Brassard, C. Crepeau, R. Jozsa, A. Peres, and W.K. Wootters, Phys. Rev. Lett. **70**, 1895 (1993).
[4] S.J. van Enk, J.I. Cirac, and P. Zoller, Phys. Rev. Lett. **78**, 4293 (1997).
[5] R. Vrijen and E. Yablonovitch, Physica E (Amsterdam) **10**, 569 (2001).
[6] A.J. Shields *et al.*, Appl. Phys. Lett. **76**, 3673 (2000).
[7] H. Kosaka *et al.*, Phys. Rev. B **65**, 201307(R) (2002).
[8] A. Rose, *Concepts in Photoconductivity and Allied Problems* (Krieger, Huntington, NY, 1978).
[9] R.H. Blick, V. Gudmundsson, R.J. Haug, K. von Klitzing, and K. Eberl, Phys. Rev. B **57**, R12 685 (1998).
[10] R.H. Blick, R.J. Haug, D.W. van der Weide, K. von Klitzing, and K. Ebert, Appl. Phys. Lett. **67**, 3924 (1995).
[11] N.C. van der Vaart *et al.*, Phys. Rev. B **55**, 9746 (1997).
[12] S. Komiyama, O. Astafiev, V. Antonov, T. Kutsuwa, and H. Hirai,

Nature (London) **403**, 405 (2000).
[13] D.D. Awschalom and J.M. Kikkawa, Phys. Today **52**, 33 (1999).
[14] H. Kosaka, A.A. Kiselev, F.A. Baron, K-W. Kim, and E. Yablonovitch, Electron. Lett. **37**, 464 (2001).
[15] A.A. Kiselev, K.W. Kim, and E. Yablonovitch, Appl. Phys. Lett. **80**, 2857 (2002).
[16] W.Y. Chou, G.S. Chang, W.C. Hwang, and J.S. Hwang, J. Appl. Phys. **83**, 3690 (1998).